Diffusion Formulation for Heterogeneous Subsurface Scattering

ADAM ARBREE, BRUCE WALTER and KAVITA BALA
Cornell University

Materials with visually important heterogeneous subsurface scattering, including marble, skin, leaves, and minerals, are common in the real world. However, general, accurate and efficient rendering of these materials is an open problem. In this short report, we describe the heterogeneous diffusion equation (DE) formulation that solves this problem. This formulation has two key results: an accurate model of the reduced intensity (RI) source, the diffusive source boundary condition (DSBC), and its associated render query function. Using there results, we can render subsurface scattering nearly as accurately as Monte Carlo (MC) algorithms. At the end of this report, we demonstrate this accuracy by comparing our new formulation to other methods used in previous work.

1. INTRODUCTION

The subsurface scattering of light creates the distinctive appearance of many ubiquitous materials, such as marble, skin, minerals and leaves. For many of these materials, the diffusion equation (DE) accurately approximates their scattering. However, to achieve this accuracy, the diffusive rendering problem must be carefully derived. This short technical report presents this derivation and demonstrates that the resulting formulation produces accurate results.

Our derivation has two key results: the diffusive source boundary condition (DSBC) and the render query function.

KEY RESULT #1: DIFFUSIVE SOURCE BOUNDARY CONDITION

The derivation of the DE makes three related approximations: the diffusion approximation (DA) that simplifies scattering in the interior of the scattering volume; a boundary condition (BC) that approximates the solution's boundary behavior; and a reduced intensity (RI) source model that approximates the radiance entering the scattering medium. The BC and RI source model strongly affect the diffusive solution on the boundary of the scattering domain. Because only the boundary is visible in an image, these approximations effectively determine the quality of the final rendering algorithm. Our first key result, the DSBC (see Equation (11)), ensures that these approximations are as accurate as possible by combining an accurate BC approximation with an improved RI source model.

KEY RESULT #2: RENDER QUERY FUNCTION

Though the DE and the DSBC fully define a diffusive scattering approximation, rendering with this approximation requires converting their solution into exitant radiance. However, because of the approximations of the DE and DSBC, this render query function must be carefully constructed to ensure accuracy. Our second key result, the render query function (see Equation (14)) provides an accurate conversion.

The rest of this report has three sections. First Sections 2 and 3 derive our two key results and then Section 4 provides a short analysis that demonstrates the accuracy of this formulation.

2. DIFFUSIVE SOURCE BOUNDARY CONDITION

The derivation of the diffusive source boundary condition (DSBC) has three parts. First, we start with an accurate Fresnel boundary condition discussed in previous work [Ishimaru 1978]. Next we augment this condition with a new term that models a diffusive boundary flux representing the reduced intensity (RI) source. Finally we apply the diffusion approximation (DA) to convert the resulting radiance constraint into a fluence constraint compatible with the diffusion equation (DE).

2.1 Fresnel Boundary Condition

The most accurate diffusive boundary condition (BC) models the behavior of the Fresnel boundary interface. At every boundary point $\mathbf{x}$, the basic condition forces the net inward flux of the solution $\Gamma_d^{\text{in}}(\mathbf{x})$ to equal the total flux of internal radiance reflected back inward by the Fresnel interface $\Gamma_d^{\text{ref}}(\mathbf{x})$.

$$\Gamma_d^{\text{in}}(\mathbf{x}) = \Gamma_d^{\text{ref}}(\mathbf{x}) \tag{1}$$

Using Figures 1(a) and 1(b) as guides, these fluxes can be computed by integrating over the small blue arrows in each figure[1].

$$\Gamma_d^{\text{in}}(\mathbf{x}) = \int_{(\vec{n}\cdot\vec{\omega})<0} L_d(\mathbf{x},\vec{\omega})(-\vec{n}\cdot\vec{\omega})\, d\vec{\omega} \tag{2}$$

$$\Gamma_d^{\text{ref}}(\mathbf{x}) = F_{dr}(\eta) \int_{(\vec{n}\cdot\vec{\omega})<0} L_d(\mathbf{x},-\vec{\omega})(-\vec{n}\cdot\vec{\omega})\, d\vec{\omega} \tag{3}$$

In Equation (3), we approximate total reflected internal flux by scaling the total exitant internal flux by $F_{dr}(\eta)$, the average Fresnel reflection coefficient.

2.1.1 *Reduced Intensity Flux.* Next, the RI source is added by augmenting the basic condition with a third term.

$$\Gamma_d^{\text{in}}(\mathbf{x}) = \Gamma_d^{\text{ref}}(\mathbf{x}) + \Gamma_s(\mathbf{x}) \tag{4}$$

The new term $\Gamma_s(\mathbf{x})$ approximates the RI source from the integrated surface radiance refracted into the material at $\mathbf{x}$.

$$\Gamma_s(\mathbf{x}) = e^{-\frac{\sigma_a(\mathbf{x})}{\sigma_s(\mathbf{x})}} \int_{(\vec{n}\cdot\vec{\omega})>0} F_t(\eta,\vec{\omega}) L(\mathbf{x},-\vec{\omega})(\vec{n}\cdot\vec{\omega})\, d\vec{\omega} \tag{5}$$

In Equation (5), the exponential term approximates the absorption that occurred as refracted radiance traveled in the medium before scattering and becoming part of the RI source.

2.1.2 *Substitution of the Diffusion Approximation.* Next, using an identity from previous work [Ishimaru 1978],

$$\int_{(\vec{s}\cdot\vec{\omega})>0} L_d(\mathbf{x},\vec{\omega})(\vec{s}\cdot\vec{\omega})\, d\vec{\omega} = \tfrac{1}{4}\Big[\phi(\mathbf{x}) - 2\kappa_d(\mathbf{x})\big(\vec{s}\cdot\vec{\nabla}\big)\phi(\mathbf{x})\Big] \tag{6}$$

we can express Equations (2) and (3) in terms of fluence by substituting the

[1] When creating these expressions, one must be careful to use a consistent definition of $\vec{\omega}$ and $\vec{n}$ to ensure that resulting boundary condition has the correct signs. To be consistent throughout this section, we have chosen to always: define $\vec{n}$ as pointing out of the material and define $\vec{\omega}$ as pointing away from $\mathbf{x}$.

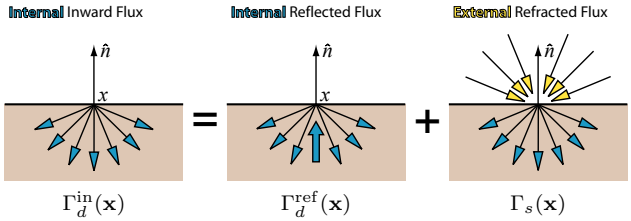

Fig. 1: Diagrams illustrating the three components of the diffusive source boundary condition (DSBC) (Equation (11)). The condition forces $\Gamma_d^{\text{in}}(\mathbf{x})$, the internal inward flux at the boundary, to be equal to the sum of $\Gamma_d^{\text{ref}}(\mathbf{x})$, the internal flux reflected at the boundary, and $\Gamma_s(\mathbf{x})$ the exterior light refracted into the material.

DIFFUSION APPROXIMATION

$$L_d(\mathbf{x},\vec{\omega}) = \frac{1}{4\pi}\phi(\mathbf{x}) + \frac{3}{4\pi}\vec{E}(\mathbf{x})\cdot\vec{\omega} \tag{7}$$

where

$$\phi(\mathbf{x}) = \int_{4\pi} L(\mathbf{x},\vec{\omega})\, d\vec{\omega} \quad \text{and} \quad \vec{E}(\mathbf{x}) = \int_{4\pi} L(\mathbf{x},\vec{\omega})\cdot\vec{\omega}\, d\vec{\omega}$$

for $L_d(\mathbf{x},\vec{\omega})$ and simplifying.

$$\Gamma_d^{\text{in}}(\mathbf{x}) = \tfrac{1}{4}\Big[\phi(\mathbf{x}) + 2\kappa_d(\mathbf{x})\big(\vec{n}\cdot\vec{\nabla}\big)\phi(\mathbf{x})\Big] \tag{8}$$

$$\Gamma_d^{\text{ref}}(\mathbf{x}) = \tfrac{1}{4}F_{dr}(\eta)\Big[\phi(\mathbf{x}) - 2\kappa_d(\mathbf{x})\big(\vec{n}\cdot\vec{\nabla}\big)\phi(\mathbf{x})\Big] \tag{9}$$

Finally, substituting Equations (8) and (9) into Equation (4) and then using the average Fresnel transmission ratio $A(\eta)$

$$A(\eta) = \frac{1+F_{dr}(\eta)}{1-F_{dr}(\eta)} \tag{10}$$

to simplify the resulting expression yields

KEY RESULT 1: DIFFUSIVE SOURCE BOUNDARY CONDITION

$$\phi(\mathbf{x}) + 2A(\eta)\kappa_d(\mathbf{x})\big(\vec{n}\cdot\vec{\nabla}\big)\phi(\mathbf{x}) = \frac{4}{F_{dt}(\eta)}\Gamma_s(\mathbf{x}) \tag{11}$$

3. QUERY FUNCTION

Given the diffusive source boundary condition (DSBC), we have a complete diffusive scattering approximation. But to complete our rendering formulation, we derive our second key result, the render query function. This function converts the solution fluence into exitant radiance. Due to the approximations of the diffusion equation (DE) and the DSBC, an accurate query function must address two computational issues. First, as the isotropy condition of the diffusion approximation (DA) breaks down, the DE solution can begin to contain erroneous angular variation. To avoid these errors, this variation must be averaged. Since, as the DA becomes more accurate, the true solution and the average solution converge [Ishimaru 1978], this averaging tends to remove artifacts without considerably increasing overall error. Second, ultimately the solution to the DE and DSBC will be computed numerically. Since for most algorithms, the numerical approximation of $\phi(\mathbf{x})$ is more accurate than a derived approximation of the fluence gradient $\vec{\nabla}\phi$, analytically removing gradient terms improves accuracy.

Together the above issues define our query function. To smooth the erroneous angular variation, the initial query averages the subsurface radiance refracted outward from the scattering material.

$$L(\mathbf{x},\vec{\omega}) = \frac{F_t(\eta,\vec{\omega})}{\pi}\int_{(\vec{n}\cdot\vec{\omega})>0} L_d(\mathbf{x},\vec{\omega})(\vec{\omega}\cdot\vec{n})\, d\vec{\omega} \tag{12}$$

Next, this initial radiance query is converted to a fluence query by substituting DA (Equation (7)) and simplifying with Equation (6).

$$L(\mathbf{x},\vec{\omega}) = \frac{F_t(\eta,\vec{\omega})}{4\pi}\Big[\phi(\mathbf{x}) - 2\kappa_d(\mathbf{x})\big(\vec{n}\cdot\vec{\nabla}\big)\phi(\mathbf{x})\Big] \tag{13}$$

Finally, we use the DSBC (Equation (11)) to remove the less accurate gradient term yielding:

KEY RESULT 2: QUERY FUNCTION

$$L(\mathbf{x},\vec{\omega}) = \frac{F_t(\eta,\vec{\omega})}{4\pi}\left[\left(1+\frac{1}{A(\eta)}\right)\phi(\mathbf{x}) - \frac{4}{F_{dt}(\eta)A(\eta)}\Gamma_s(\mathbf{x})\right] \tag{14}$$

4. RESULTS

To end this short report, we demonstrate that this formulation renders accurate images. This section has three parts. First, we describe the rendering environment used to produce these results. Second, we demonstrate that our formulation produces nearly exact solutions by comparing our results to images produced with a Monte Carlo (MC) path tracer. Finally, we discuss how this solution can be used to correct errors found in the recent previous work by Wang et al. [2008].

4.1 Details of the Rendering Computation

All results were generated on a 8 x 2.66Ghz Xeon workstation with 8GB of RAM. All images are 640x480 pixels and each is 16x anti-aliased. For all images, we compute the surface and single scattering components separately using a combination of Multidimensional Lightcuts (MDLC) [Walter et al. 2006] and an analytical single scattering approximation [Hanrahan and Krueger 1993]. The multiple scattering is solved by computing a numerical solution to our heterogeneous diffusion formulation. We use an accurate finite element (FE) algorithm for this purpose.

4.2 Comparison with Monte Carlo

Demonstrating the quality of our algorithm, Figure 2 compares our solution for a Dragon test scene with the same image produced by an exact, MC path tracer. To facilitate the quality comparison, an absolute error image is provided. Since these error images are nearly black, a 4x magnified versions help reveal three differences. There are two principle differences. First, particularly prominent in the tail, the path tracer is able to capture highlights from caustic paths that do not scatter within the material. However, since these caustic paths are not part of the subsurface scattering, this is an error of our MDLC surface render not our FE algorithm. Second, because the diffusion equation (DE) treats all diffusive radiance as nearly isotropic, it tends to overestimate the frequency of scattering in thin geometry and near the surface and, as a consequence, it underestimates contributions from low order scattering events. This slightly darkens regions when they are lit from behind as in the optically thinner parts of the Dragon. However, overall, these differences are small and result from limitations in our diffusion approximation (DA). The new

Our Solution Path Tracing

Fig. 2: Using our formulation produces images nearly identical to path traced references (see black difference images; right).

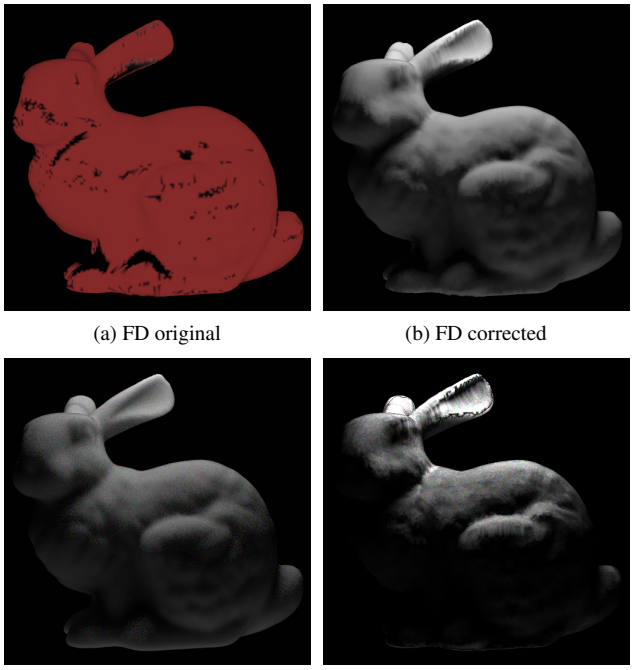

(a) FD original (b) FD corrected

(c) MC (d) 4x FD error

Fig. 3: Images of a constant scattering white bunny lit by two area lights, fill below and key above: Figure 3(a) as described in Wang et al. [2008] with negative radiance areas highlighted in red; Figure 3(b) corrected using our formulation; Figure 3(c) MC reference; and Figure 3(d) 4x absolute error of Figure 3(b).

elements of our formulation add little additional error and ensure surprisingly accurate results.

4.3 Correction of Wang et al. [2008]

Next we demonstrate that this formulation corrects errors in the solution used in the previous heterogeneous rendering algorithm by Wang et al. [2008]. Since here our focus is accuracy, rather than performance, we produced our test images using a software version of their iterative finite difference (FD) algorithm. This software renderer omits the multi-resolution approximation originally required

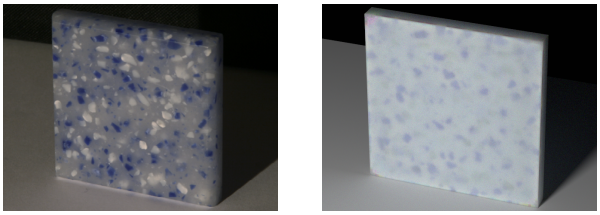

Photograph Path tracing

Fig. 4: Comparison of the photograph artificial stone slab captured by Wang et al. [2008] to a path traced rendering of the resulting material parameters.

by their method to achieve interactive performance. We allow the FD algorithm to update fully each step and iterate until the solution is converged thus maximizing their solution's quality in our comparison.

To facilitate our tests, Wang et al. [2008] kindly provided their measured material data and a PolyGrid [Tarini et al. 2004] bunny model. Using the PolyGrid, we created several images of the bunny with a white, homogeneously scattering material (see Figure 3). Because their solution uses an incorrect version of the diffusive source boundary condition (DSBC) and render query function, their original algorithm sometimes computes negative radiance values. As demonstrated in red in Figure 3(a), this happens almost everywhere on the homogeneous bunny. However, our new formulation can correct this error. The rest of images in Figure 3 directly compare, Wang et al.'s FD algorithm and a path traced reference (Figures 3(b), 3(c) and 3(d) respectively).

We believe that in the original work, this error was invisible because their capture optimization corrects errors by altering the computed material parameters. To test this hypothesis, we rendered the artificial stone material captured by Wang et al. [2008] using a path tracer and compared the result to a photograph of the original material (see Figure 4). Though we are unsure of the exact mechanism, the large difference between the two results indicates that the measured parameters are not physically accurate.

5. CONCLUSION

In this technical report, we presented a high-quality rendering formulation for the heterogeneous diffusion problem. Our formulation has two key results: the correct boundary condition, the diffusive source boundary condition (DSBC) (Section 2), and a query func-

tion that converts the diffusion solution to exitant radiance (Section 3). We show that this new formulation can produce results nearly as accurate as Monte Carlo (MC) solution (Section 4.2) and that it can be used to improve the previous diffusion algorithm by Wang et al. [2008] (Section 4.3).

ACKNOWLEDGMENTS

We would like to thank the authors of Wang et al. [2008]—Jiaping Wang, Shuang Zhao, Xin Tong, Stephen Lin, Zhouchen Lin, Yue Dong, Baining Guo and Heung-Yeung Shum—whose help, both for supplying material models and PolyGrid meshes, was invaluable when creating the comparisons presented here.

REFERENCES

HANRAHAN, P. AND KRUEGER, W. 1993. Reflection from layered surfaces due to subsurface scattering. In *SIGGRAPH '93: Proceedings of the 20th annual conference on Computer graphics and interactive techniques*. ACM, New York, NY, USA, 165–174.

ISHIMARU, A. 1978. *Wave Propagaion and Scattering in Random Media*. Academic Press.

TARINI, M., HORMANN, K., CIGNONI, P., AND MONTANI, C. 2004. Polycube-maps. In *SIGGRAPH '04: ACM SIGGRAPH 2004 Papers*. ACM, New York, NY, USA, 853–860.

WALTER, B., ARBREE, A., BALA, K., AND GREENBERG, D. P. 2006. Multidimensional lightcuts. In *SIGGRAPH '06: ACM SIGGRAPH 2006 Papers*. ACM, New York, NY, USA, 1081–1088.

WANG, J., ZHAO, S., TONG, X., LIN, S., LIN, Z., DONG, Y., GUO, B., AND SHUM, H.-Y. 2008. Modeling and rendering of heterogeneous translucent materials using the diffusion equation. *ACM Trans. Graph. 27,* 1, 1–18.